Hindawi
Advances in Materials Science and Engineering
Volume 2022, Article ID 4975059, 14 pages
https://doi.org/10.1155/2022/4975059

Research Article

Influence of Stone Shape Factor on the Pull-Out Resistance of Geogrid in the Soil-Rock Mixture

Yongshuai Sun,[1] **Xuefeng Li**,[2] **and Guihe Wang**[2]

[1]*College of Water Resources & Civil Engineering, China Agricultural University, Beijing 100083, China*
[2]*School of Engineering and Technology, China University of Geosciences, Beijing 100083, China*

Correspondence should be addressed to Yongshuai Sun; cugbsys@163.com

Received 27 May 2022; Accepted 4 July 2022; Published 22 July 2022

Academic Editor: Ivan Giorgio

In this paper, the particle shape factor of the stone in the soil-rock mixture was used as the specific research object of the geogrid pull-out test, combining the random generation method and evaluation criteria of rock blocks in the soil-rock mixture, and a feasible method for classifying stones according to their shape factors is presented. By comparing the mechanical behavior of soil-rock mixture composed of rock blocks with different rock material shape factors in the geogrid pull-out tests under different working conditions, we studied its changing laws. The research shows that with the increase of the shape factor of the stone, the pull-out resistance of the geogrid gradually decreases. When the stone paved in the model box changes from a single layer to a double layer, the pull-out resistance of the geogrid increases, and there is a disturbance range in the contact interface between the geogrid and the stone; stone blocks 5 cm away from the geogrid surface can still have an indirect effect on the pull-out resistance of geogrids; the pull-out resistance of geogrid in clay is greater than that in the sand; and an empirical expression for predicting the pull-out resistance of geogrids is obtained. This empirical expression helps to explain the influence mechanism of stone shape on drawing resistance of geogrid.

1. Introduction

Soil-rock mixture is a geological body composed of gravel or stone as aggregate and clay or sand as filler [1]. It is often used in conjunction with reinforced materials and is widely used in engineering fields. As a subgrade foundation and abutment foundation in highway and railway engineering [2, 3], and in traffic construction, the soil-rock mixture can be reinforced to achieve the purpose of crack resistance of the pavement [4, 5]. When replacing and filling the foundation, the soil-rock mixture of natural grading or artificial grading is often used as replacement filling [6, 7]. When high-fill retaining walls are required in wharf projects, large-scale slag fields, and coal mining, reinforced soil retaining walls with the soil-rock mixture as filler are also common composite support methods [8–10].

Scholars have done considerable research on the soil-rock mixture, research contents included: establishing a regression equation to predict the uniaxial compressive strength of mixed rocks [11–13], proposed a generalized empirical expression which is used to predict the overall strength of uncemented soil-rock mixture [14–17], controlled the influence of different factors on direct shear test results of soil-rock mixture [18–21]. The shape of the stone is an important factor affecting the properties of the soil-rock mixture, academic circles study by quoting the particle shape factor [22–30]: obtained and calculated the particle shape factors and angular angles of the soil-rock mixture through 3D scanning, and the related experiments were simulated, used image recognition technology, combined with geostatistical methods, the mechanical parameters of the geological body were found to be correlated with the rock blocks shape.

Minuto and Morandi [31] proposed the concept of "reinforcement of soil-rock mixture" In the study of the interaction mechanism of the reinforcement-soil interface, the pull-out test has been widely used as an important research method [32–37]. The pull-out test focus on the

deformation characteristics of the geogrid, study the difference in strain between the front and rear parts of the grid [38–42], study the contribution rate of horizontal and vertical reinforcement [43–46], so that the grid must be simulated with a clump in the numerical simulation test [43, 47, 48]. Research shows that [49, 50] there is a disturbance range in the contact interface between the geogrid and the fill, and this disturbance range is asymmetric up and down.

In this study, the particle shape factor of the stone in the soil-rock mixture was used as the specific research object of the geogrid pull-out test, combining the random generation method and evaluation criteria of rock blocks in the soil-rock mixture, and compared the mechanical behavior of soil-rock mixture composed of rock blocks with different rock material shape factors in the geogrid pull-out tests under different working conditions, and studied its changing laws. For exploring the ways to parametrically classify real stones by shape, start with real stones, instead of starting with virtual random model building, and accomplish the parametric control of the shape of the stone, then, the purpose of retaining the true shape of the stone and parametric control of the stone shape can be achieved.

2. Determination Test of the Stone Shape Factor of Soil-Rock Mixture

2.1. The Principle of the Coating Method. In this paper, the coating method was used to determine the stone shape factor of two batches of boulders. In the first batch of boulders, the causes of errors were analyzed, and in the second boulders, the tools and coating materials were changed. The difference between the two determination results was compared and analyzed, and the determination method of the stone shape factor of the soil-rock mixture was improved.

The shape factor of a rock block is the ratio of the actual area of the particle surface to the surface area of a sphere of the same volume. The essence of this factor is that when a three-dimensional closed shape expands or shrinks by the same multiple in all directions of space, its particle shape factor remains unchanged. The particle shape factor is a comprehensive reflection of the overall slenderness ratio and roundness of the rock block. This factor has an important influence on the compactness and internal friction angle of the soil-rock mixture and can be simply and effectively be determined for the mesoscopic structure of the generated rock block for evaluation and classification.

The coating method is a method of "setting and not seeking" the shape factor of the rock material. The rock material shape factor is expressed as follows:

$$\xi = \frac{S}{4\pi\left(3V/4\pi\right)^{2/3}}. \tag{1}$$

S is the actual surface area of the stone; V is the volume of the stone.

The mass of the stone is $m1$ and the density of the stone is $\rho 1$; then, the volume of the stone is as follows:

$$V = \frac{m_1}{\rho_1}. \tag{2}$$

Note that the mass of the stone after the painting is $m2$, the density after the paint is completely dried is $\rho 2$, and its thickness is h; then, the surface area of the stone is

$$\begin{aligned} S &= \frac{m_1 - m_2}{\rho_2 h}, \\ \xi &= (4\pi)^{-1/3} 3^{-2/3} \rho_1^{2/3} \rho_2^{-1} h^{-1} \left(\frac{m_1 - m_2}{m_1^{-2/3}}\right). \end{aligned} \tag{3}$$

Considering C is a constant, then

$$\xi = C\left(\frac{m_1 - m_2}{m_1^{-2/3}}\right), \tag{4}$$

where the constant C is a function of the paint density, the average thickness of paint applied to the stone, and the amount of stone density, it is difficult to measure these three quantities, and it does not measure it and does not affect the subsequent experiments. Therefore, in this experiment, the constant C is not measured; consider,

$$\zeta = \left(\frac{m_1 - m_2}{m_1^{-2/3}}\right). \tag{5}$$

When an object of a certain shape expands times in the X, Y, and Z directions at the same time, then its surface area will expand $a2$ times and its volume will expand $a3$ times; when a three-dimensional closed surface is expanded by times in the X, Y, and Z directions at the same time, its rock material shape factor ξ remains unchanged; this is the essence of the rock material form factor. In the expression of ζ, the part representing the surface area and the part representing the volume are in a 2/3 power relationship, so ζ is still a number that characterizes the properties of particles. Based on the above discussion, in this experiment, we decided not to determine the rock material shape factor ξ, instead, use ζ indirectly, hereinafter referred to as ζ as the shape eigenvalue.

2.2. Test Materials and Procedures. Select the stone particle size between 20 mm−40 mm, to better reflect the randomness of the stone shape, the stones selected in this experiment were broken from un-weathered hypabyssal intrusive rocks, the texture is hard and uniform, which ensures the randomness of the shape of the stone after crushing to a certain extent. The first batch of rock materials measured in the test used silver paste enamel and barite powder as the coating material, and the second batch of measured materials used oil-based quick-drying paint as the coating material.

Number each stone and place it neatly in numbered order. The sequence of rock material numbers is shown in Figure 1. Weigh the mass $m1$ of each stone. Take silver paste enamel 400 ml, weigh barite powder 100 g, add it to the weighed silver paste enamel, stir well, put the stones into the utensils filled with paint in numbers, stir to make the paint

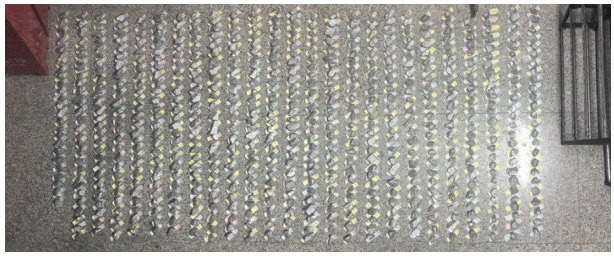

Figure 1: Sorting of rock material numbers.

cover the surface of the stones, take them out and place them on the ground in order of number to ventilate and dry, after 48 hours, weigh the mass $m2$ of each stone in the order of numbers, calculate the particle shape characteristic value of each stone block, and group the stone blocks according to the particle shape characteristic value division rules for subsequent experiments.

2.3. Improvement Measures of the Coating Method. During the preliminary test, the recipe uses silver paste enamel and barite as a coating, (400 ml silver paste enamel + 100 g barite powder), the purpose of adding barite is to increase the coating density and reduce the resolution pressure of the electronic scale. The stones in Figure 2 are arranged by number, stones leftover during reordering by shape eigenvalues, if these stone shape eigenvalues are randomly distributed, then the stones that have been selected and the remaining stones will be evenly distributed, but the fact is that the remaining stones are aggregated in several sections, it also means that the shape eigenvalues measured by the numbered stones in this section are too large as a whole. Therefore, in this test, the oil-based quick-drying paint without thinner is used as the coating material, after testing, this kind of paint will not have the sorting and enrichment of components during the painting process, it can even cover the entire surface of the stone, and re-stores the characteristics of high viscosity at rest, the phenomenon that the coating is "thin on the top and thick on the bottom" during the hanging and drying process of the stone blocks is improved.

A total of 650 stones were processed in the first batch, and the first batch of rock material shape' eigenvalues is mainly distributed between 21 and 34. The distribution of the number of rocks contained in each shape eigenvalues measured is shown in Figure 3.

A total of 564 rocks were processed in the second batch and the distribution of the number of stones contained in each shape eigenvalues measured is shown in Figure 4.

Comparing the particle shape eigenvalues measured by the two methods, it can be found that the results obtained by the improved test method have a smoother variation law, and the measurement results are more accurate. In subsequent experiments, it is necessary to control the stone content of the soil-rock mixture to remain unchanged, the rock content of the soil-rock mixture in each pull-out test is set as a constant, considering the cross-sectional size of the model box and the number of geogrid grids, it is determined

Figure 2: The collective largeness of the rock material shape factor.

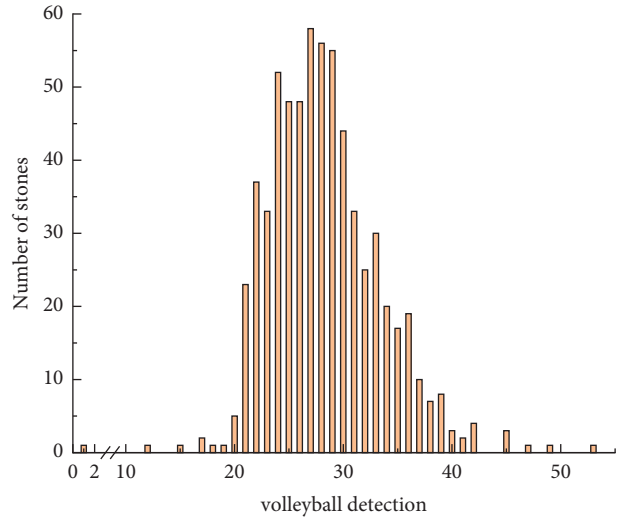

Figure 3: Distribution of eigenvalues of rock material shape-1.

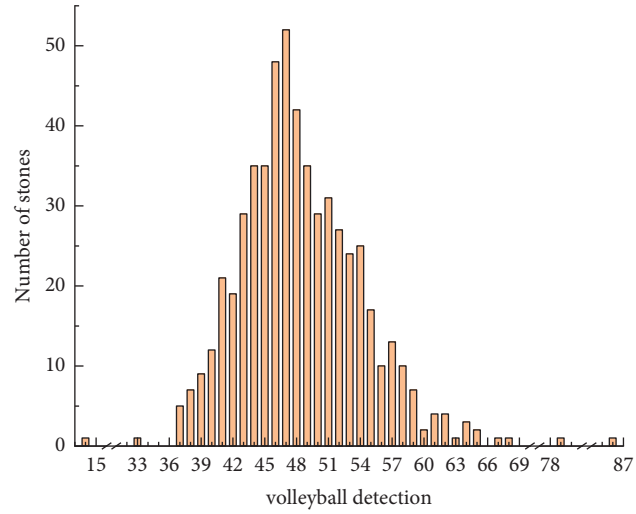

Figure 4: Distribution of eigenvalues of rock material shape-2.

that the total mass of stones laid in a single layer is 1.65 kg, the thickness of each layer is 5 cm, in this way, the soil-rock mixture is used as the test object, and its rock content is

fixed. Table 1 counts the number of stones with different shape eigenvalues and same quality:

It can be seen from the statistical results that with the increase of the characteristic value of the shape of the stone, the number of stones of the same quality is gradually increased, and the particle size of the stone is between 20 mm and 40 mm. Looking back at the previous test steps, the particle size of the stones was not sorted, and the distribution of the stone particle size in each grouping of the shape eigenvalues was still random. Therefore, it can be inferred from Table 1 that the coating method can effectively sort the stone shape.

Table 1: Comparison of the number of stones of the same quality.

Shape factor	Quality (kg)		
	1.65	3.3	6.6
9–24	40	72	150
25–27	38	76	150
28–30	43	86	176
31–34	50	99	198

3. Pull-Out Test of Soil-Rock Mixture

In the pull-out test, the eigenvalues of the shape of the stone, the type of the matrix soil, and the layer thickness of the soil-rock mixture were used as the test variables, 16 pull-out tests of geogrids filled with soil-rock mixture were carried out, two reference tests were also carried out, one with clay and one with sand.

3.1. Test Device. The pull-out test adopts the self-developed pull-out instrument as shown in Figure 5. The internal clearance of the pull-out box is 500 mm × 370 mm × 300 mm. A pull-out joint with 300 mm width and 5 mm height is left on the loading end plate as the pull-out outlet of the geogrid. The geogrid fixture in this test consists of two steel plates, sandwiching the geogrid, then fastened with six 8 mm diameter screws. The two openings on the top are used to connect the retaining ring to the sensor. In the drawing process, the friction force transmission between geogrid and steel plate avoids the uneven stress of geogrid longitudinal reinforcement. Considering the biting effect of geogrid and stone, as the geogrid is pulled out, the stone will be stuck at the outlet of the slit on the steel plate. Therefore, the box body is not filled with stone within 100 mm from the front box surface, but only filled with clay or sand, that is, the displacement stroke of the designed geogrid is 100 mm. The reinforcement material is polypropylene plastic two-way geogrid (TGSG5050). The main technical parameters are shown in Table 2.

In the test, the support reaction is applied on both sides of the geogrid outlet on the front surface of the model box, so that the model box does not deflect or slide without fixing. The drawing power part is provided by an electric push rod with a maximum thrust of 5000 N, powered by 24 V DC, and the propulsion speed is 3 mm/s–5 mm/s. The square S-type tension-compression bi-directional sensor is selected, and the maximum range is 2 T. The analog signal can be converted to a digital signal through the signal conversion module, and the tension value can be displayed with the weighing software.

3.2. Test Material. A soil-rock mixture is an extremely uneven geological body consisting of gravel or blocks of stone as aggregate and fine-grained soil or sand as filler, a major feature of the soil-rock mixture is the discontinuity of

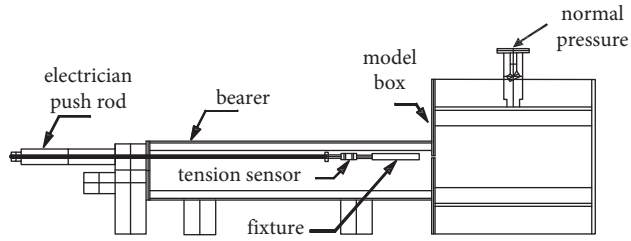

Figure 5: Test device.

particle size gradation, the particle size gap between large and small particles is large, and there is no transition particle size in the middle. To better reflect the concept of this soil-rock mixture, in this experiment, the abovementioned rock material classified by shape factor were selected, the particle size is between 20 mm–40 mm, the particle size is kept below 0.05 mm, at the same time, the moisture content of the soil-rock mixture is set to 0, it can be ensured that the clay particle size will not agglomerate and cause particle size changes during repeated tests.

The yellow sand selected in this test is fine sand with a particle size between 0.1 mm and 0.2 mm, the stones are those prepared by the method described above, to better reflect the randomness of the stone shape, the stones selected in this experiment were broken from unweathered shallow intrusive rocks. In layered structures without sedimentary rocks, there is also no obvious flow structure or joints, the texture is hard and uniform, which ensures the randomness of the shape of the stone after crushing to a certain extent.

3.3. Test Scheme. The stones with different stone shape factors were divided into 4 groups as experimental variables. Due to the different coating compositions used in the two batches of stones, the distribution range of the eigenvalues of the stone shape is different, the solution is to do a linear conversion of the shape eigenvalues of the second batch of stones, equivalent to the first batch of stones. First, equate the two peaks, the eigenvalue 27 of the first batch of stones is equivalent to the eigenvalue 47 of the second batch of stones, then divide the variable grouping of shape factor according to the same percentage of the number of stones in the total batch. The soil types are divided into two types: clay and sand. The layer thickness of the soil-rock mixture is set to 10 cm and 20 cm.

According to the division and setting of the above test variables, the following experimental protocol was developed (see Table 3), with two groups of experiments without the addition of stones serving as control experiments:

Table 2: Geogrid parameters.

Grid size (length, width) (mm)	Transverse rib width (mm)	Longitudinal rib width (mm)	Transverse rib thickness (mm)	Longitudinal rib thickness (mm)	Node thickness (mm)
30, 30	2.0	2.0	1.7	1.5	4.5

Table 3: Pull-out test scheme.

Test number	The eigenvalue of stone shape	Filler type	Layers and thickness of stone laying
1	—	Clay	—
2	9–24	Clay	Monolayer (100 mm)
3	9–24	Clay	Double layer (200 mm)
4	25–27	Clay	Monolayer (100 mm)
5	25–27	Clay	Double layer (200 mm)
6	28–30	Clay	Monolayer (100 mm)
7	28–30	Clay	Double layer (200 mm)
8	31–34	Clay	Monolayer (100 mm)
9	31–34	Clay	Double layer (200 mm)
10	—	Sand	—
11	9–24	Sand	Monolayer (100 mm)
12	9–24	Sand	Double layer (200 mm)
13	25–27	Sand	Monolayer (100 mm)
14	25–27	Sand	Double layer (200 mm)
15	28–30	Sand	Monolayer (100 mm)
16	28–30	Sand	Double layer (200 mm)
17	31–34	Sand	Monolayer (100 mm)
18	31–34	Sand	Double layer (200 mm)

4. Test Results and Analysis

4.1. Pull-Out Test of Clay-Soil-Rock Mixture. Before carrying out the pull-out test of soil-rock mixture with clay as the matrix, first, a clay pulling test without adding stones was carried out as a reference; the curve of its pulling resistance with time is shown in Figure 6.

It can be seen from Figure 6 that in the clay, the pulling resistance increases rapidly at first, the maximum value was 1600 N, after reaching the peak, the pulling resistance gradually decreased, and was stable at around 700 N in about 10 s.

In the soil-rock mixture, the matrix was clay; when laying stones in a single layer (10 cm), four groups of tests were performed on four groups of stone shape factors (9–24, 25–27, 28–30, 31–34); the numbers were 1-1, 1-2, 1-3, and 1-4, respectively, and the curve of the pulling resistance with time is shown in Figure 7.

In test 1-1, the tensile force first increased rapidly to a peak value of 1950 N, after the geogrid was pulled out, the contact area between the geogrid and the soil-rock mixture was reduced, and the pull-out resistance gradually decreases. Before the trial was terminated, the pulling force has an obvious second peak of 1770 N, at the end of the test, the tension was stable at 1600 N; in test 1-2, the first peak of the tension was 1830 N, smaller than trial 1, the second peak of 1200 N also appeared between 13 and 15 s, at the end of the test, the tension was stable at 1060 N; in test 1-3, the first peak of the tension was at 1650 N, compared with experiment 2, it continued to decrease, and the second peak of 1330 N appeared between 12 and 13 s, the tension at the end of the test was 1180 N; in trial 1-4, the performance of tension was similar to that of geogrid in pure clay, there was only one peak in the pull-out resistance, and that peak was at 1510 N, below the peak value of 1600 N in the pure clay test, there was no obvious second peak, however, the tensile force at the end of the test was still higher than that at the end of the pure clay test, which was 1030 N.

In the soil-rock mixture, the matrix was clay; when laying stones in double layers (20 cm), four groups of tests were performed on four groups of stone shape factors (9–24, 25–27, 28–30, 31–34); the numbers were 2-1, 2-2, 2-3, and 2-4, respectively; and the curve of the pulling resistance with time is shown in Figure 8.

When the distribution layer thickness of the stones in the soil-rock mixture was doubled, the pulling resistance provided by the soil-rock mixture increased accordingly, during the drawing process, the double-peak phenomenon of the pulling force still existed.

In test 2-1, the first peak was at 2720 N, and the second peak of 2720 N appears clearly between 9 and 10 s, Equivalent to the first peak, the full force at the end of the test was at 2350 N; in test 2-2, the first peak was at 1720 N, and the tension gradually decreased and then gradually increased to the second peak of 1760 N. In this test, the second peak was higher than the first peak for the first time, and the tension was 1620 N at the end of the test; In 2-3, the first peak of the tension was at 1800 N, and then, the tension gradually decreased to 1200 N. At 13-14 s, the tension fluctuated once, but there was no obvious peak; in test 2-4, the first peak of the tension was at 1490 N, lower than the maximum tension of the clay pull-out test of 1600 N, in the process of gradually decreasing the tension after reaching the peak value, the curve shows an upward convexity, which is different from other tests. The second

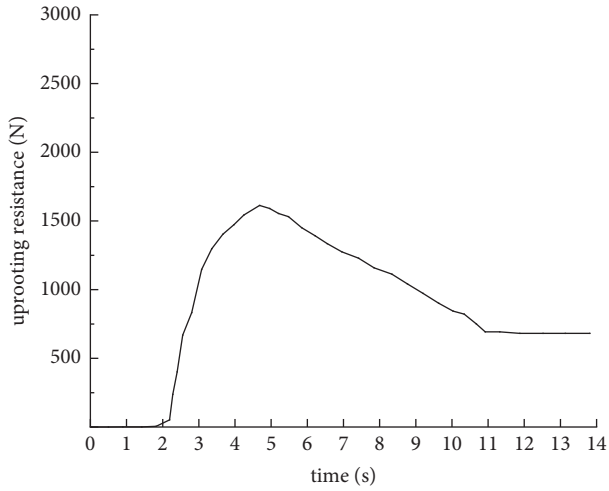

Figure 6: Clay pull-out test.

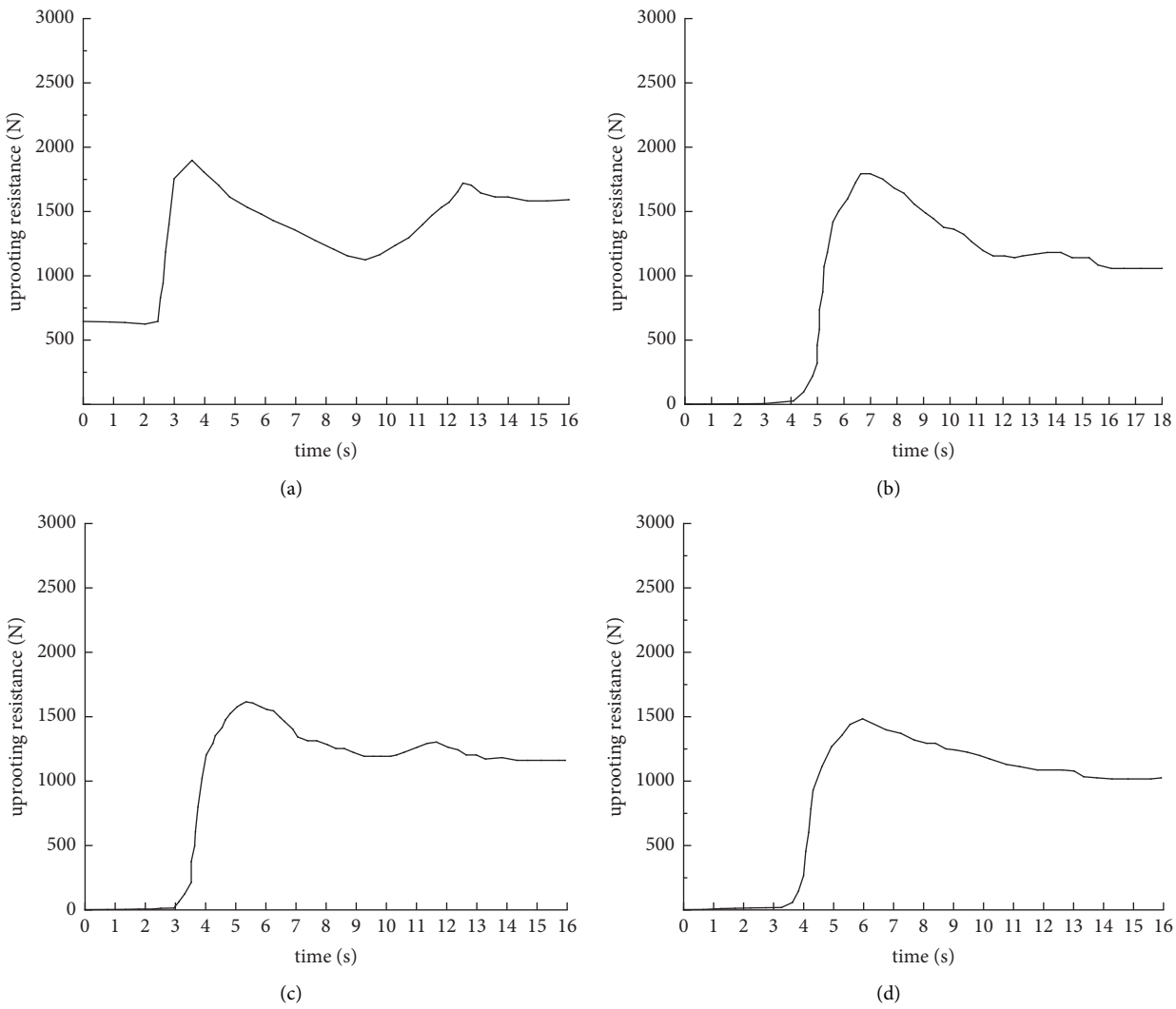

Figure 7: Clay matrix, single-layer stone test results. (a) Test 1-1. (b) Test 1-2. (c) Test 1-3. (d) Test 1-4.

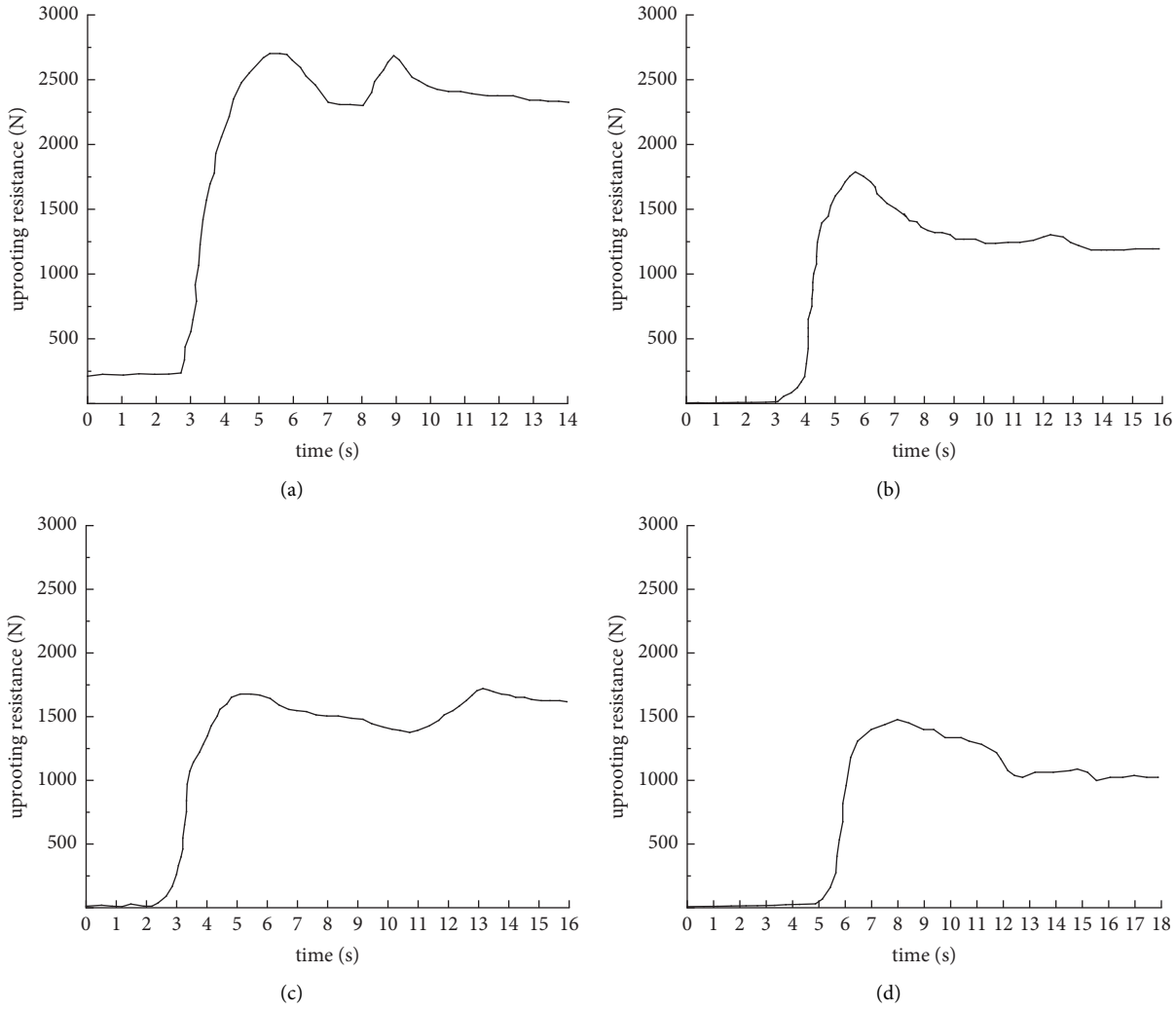

Figure 8: Test results for clay matrix, double-layer stone. (a) Test 2-1. (b) Test 2-2. (c) Test 2-3. (d) Test 2-4.

peak that appeared was at 1110 N, and the tension value at the end of the test was 1020 N.

It can be seen that compared with the pull-out test of clay as a reference, the representative values of pull-out forces of test 1-1, 1-2, 1-3, 2-1, 2-2, and 2-3 were higher than those of reference test, and the representative values of pull-out forces of test 1-4 and 2-4 were lower than those of reference test.

4.2. Sand-Soil-Rock Mixture Pull-Out Test. Before carrying out the pull-out test of the soil-rock mixture with sand as the matrix, first, the sand pulling test without adding stones was carried out as a reference. The curve of its pull-out resistance with time is shown in Figure 9.

Compared with the pull-out test of clay, the pull-out test of sand has the following characteristics:

(1) The overall tension value is low, the maximum tension value is 1420 N, it is lower than the peak tension of the clay test of 1600 N, and the tension value at the end of the test was 1240 N;

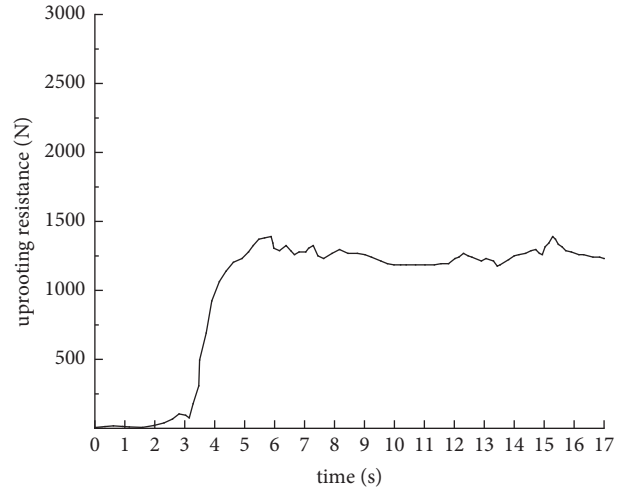

Figure 9: Sand pulling test.

(2) During the whole drawing process, there is no obvious change in the peak of the tension and the increase or decrease of the tension value;

(3) In the pull-out test of clay and the pull-out test with clay as the matrix, the change curve of the tensile force value is "smooth." The pull-out test curve appears to be "rough," which is a characteristic of sand pull-out tests.

In the case that the soil-rock mixture matrix is sand and the paving stones are a single layer (10 cm), the four groups (9–24, 25–27, 28–30, 31–34) of the stone shape factors were tested for four group test, the numbers are 3-1, 3-2, 3-3, and 3-4, respectively, and the curve of the pull-out resistance with time is shown in Figure 10.

In test 3-1, the tensile force first rapidly increased to a peak value of 1580 N, then, with the pull-out of the geogrid, the contact area between the geogrid and the soil-rock mixture decreased, and the pull-out resistance gradually decreases. Before the end of the test, there was an obvious second peak of 1580 N in the tensile force. When the test was terminated, the tensile force was stable at 1410 N; in tests 3-2, the first peak value of the tension was at 1400 N, and the tension does not show a gradual decrease trend after reaching this value. Instead, it stabilized at this level for 5 s, after which the tension value continued to increase, reaching a peak value of 2190 N, and the tension stabilized at 1950 N at the end of the test; in test 3-3, the change law of the tension curve is the same as in test 3-2, the overall tension value was small, and the stable time reaches 5s after reaching the first peak value of 1140, and then, the tension value continues to increase to the second peak value of 1340 N, and the test was over when the tension value was 1220 N; in test 3-4, the change law of the tension curve is similar to that of test 3-3. After reaching the first peak value of 1300 N, the stability time was 5 s, and then, the tension value continues to increase to the second peak value of 1580 N. At the end of the test, the tension value is 1410 N.

In the soil-rock mixture, matrix is sand, when laying stones in a single layer (20 cm), four groups of tests (9–24, 25–27, 28–30, 31–34) of stone shape factors were carried out, and their numbers were 3-1, 3-2, 3-3, 3-4. The curve of the pulling resistance changing with time is shown in Figure 11.

In test 4-1, the tension first rapidly increased to a peak value of 1420 N, and then with the pull-out of the geogrid, the tension decreased, and before the test was terminated, the second peak of the tension was at 1400 N, at the end of the test, the tension was stable at 1240 N; in test 4-2, the tension did not show the first peak, instead, the growth rate of the pulling force changed from rapid growth to becoming stable. The pulling force value at this inflection point is 1340 N, after the tension reached this value, it did not show a trend of gradual decrease, but stabilizes at this level for 5 s, after which the tension value continues to increase, reaching a peak value of 1960 N, and the tension was stable at 1610 N at the end of the test; in test 4-3, the change law of the tension curve was the same as that of the sand pulling test, the overall tension value was small, and it stabilized after reaching the inflection point of 1320 N until the end of the test, and the tension value at the end of the test was 1250 N; in test 4-4, the changing law of the tension curve was similar to that in test 4-3, it was stable after reaching the inflection point of 1390 N until the end of the test, and the tension value at the end of the test was 1310 N.

It can be seen that compared with the pull-out test of sand as a reference, the representative values of the pull-out force of test 3-1 and 3-2 were higher than those of the reference test. The representative value of the pull-out force of test 4-1 was equal to that of the reference test, and the representative values of the pull-out force of other tests were lower than those of the reference test.

The first peak value of each pull-out test was selected as the representative value of the pull-out test pull force in this test; if the curve appears to stabilize after reaching a certain level, the first peak did not appear, but an "inflection point" appeared; select this "inflection point" as the representative value of the pull test tension, and tensile force representative value (N) of pull-out test is shown in Table 4.

Through the 16 tests, the following expression is obtained as an empirical expression to predict the pull-out force of the geogrid pull-out test conducted in the soil-rock mixture:

$$F = (56.2m - 47.8n - 91.2mn + 44.8)(S - 4.77) + 1258.6. \quad (6)$$

The relationship between the parameters in the formula is linear, where F is the pull-out force of the geogrid; m is the layer thickness parameter of the soil-rock mixture, which is 1 when the layer thickness is 10 cm, and 2 when the layer thickness is 20 cm; n is the parameter of the matrix soil type, which is 2 when the matrix is clay, and 1 when the matrix is sand; S is the grouping number of the stone shape factor, which is 1, 2, 3, and 4, respectively.

According to the analysis of Figure 12 and the empirical formula for predicting the drawing force, it can be concluded that the maximum drawing resistance provided by the soil-rock mixture gradually decreases with the increase of the stone shape factor, and the drawing force of the double-layer soil-rock mixture is larger than that of the single-layer soil-rock mixture. The representative value of the drawing force in the soil-rock mixture with sand as the matrix is 6%–20% less than that of the soil-rock mixture with clay as the matrix.

Before the pull-out test, constant pressure was applied to the top plate of the model box with a press to achieve a certain degree of consolidation of the soil-rock mixture. However, during the pull-out test, the normal pressure applied on the roof of the model box is unloaded, and the roof of the model box will tilt. Under different test conditions, the inclination angle of the top plate is different. The record of inclination angle of the top plate at the end of the test is as shown in Table 5.

The line chart of the tilt angle of the top plate is as follows:

Figure 13 shows that with the increase of the shape factor, the inclination angle of the roof of the model box in the clay matrix decreases gradually, and in the sand matrix, the roof of the model box decreases first and then increases, and the inclination angle of the roof of the model box with clay as filling material is less than that of the sand as filling material. In the test, the inclination angle of the roof of the

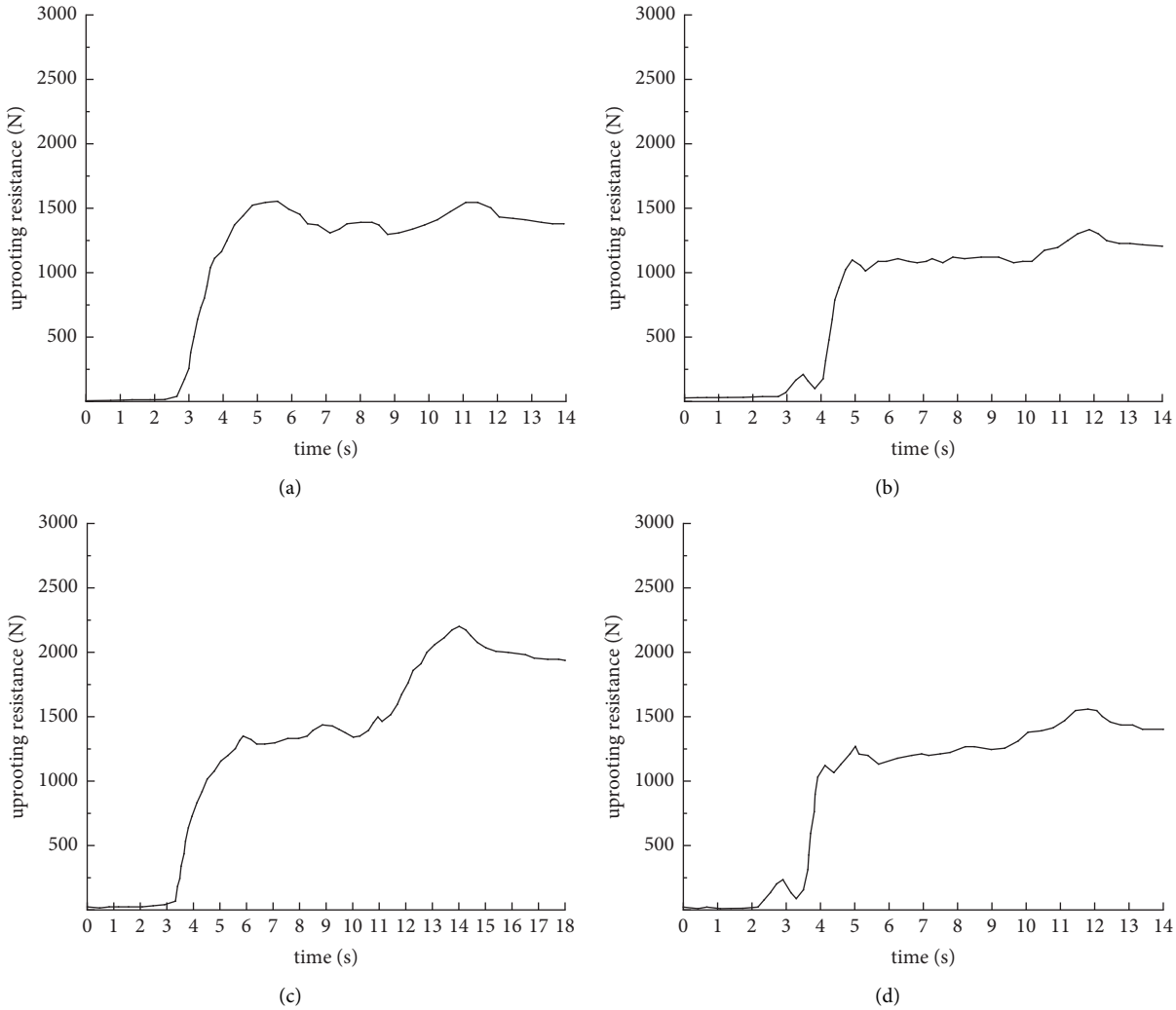

Figure 10: Sand matrix, single-layer stone test results. (a) Test 3-1. (b) Test 3-2. (c) Test 3-3. (d) Test 3-4.

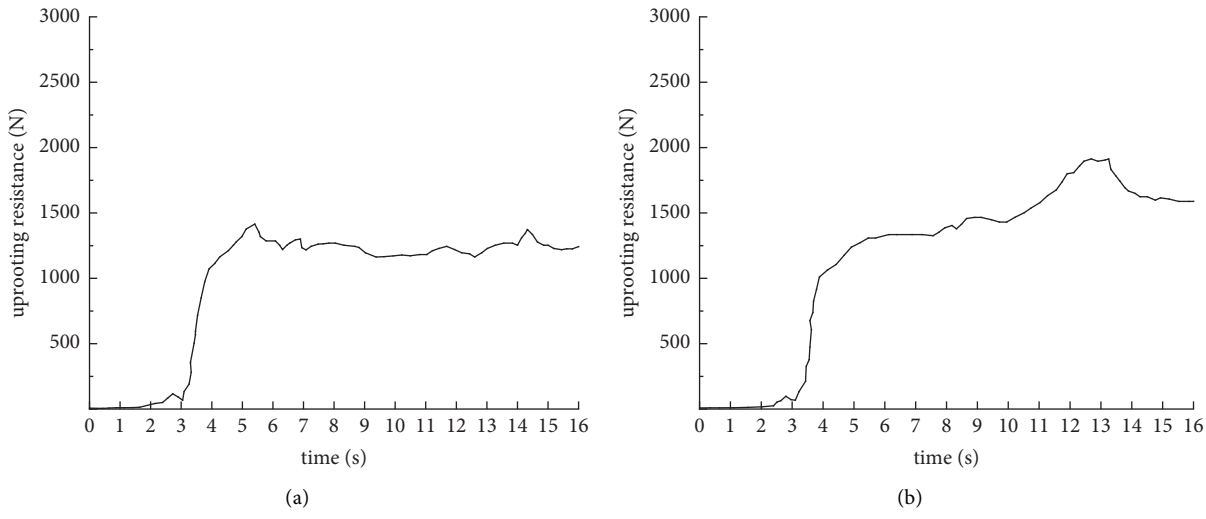

Figure 11: Continued.

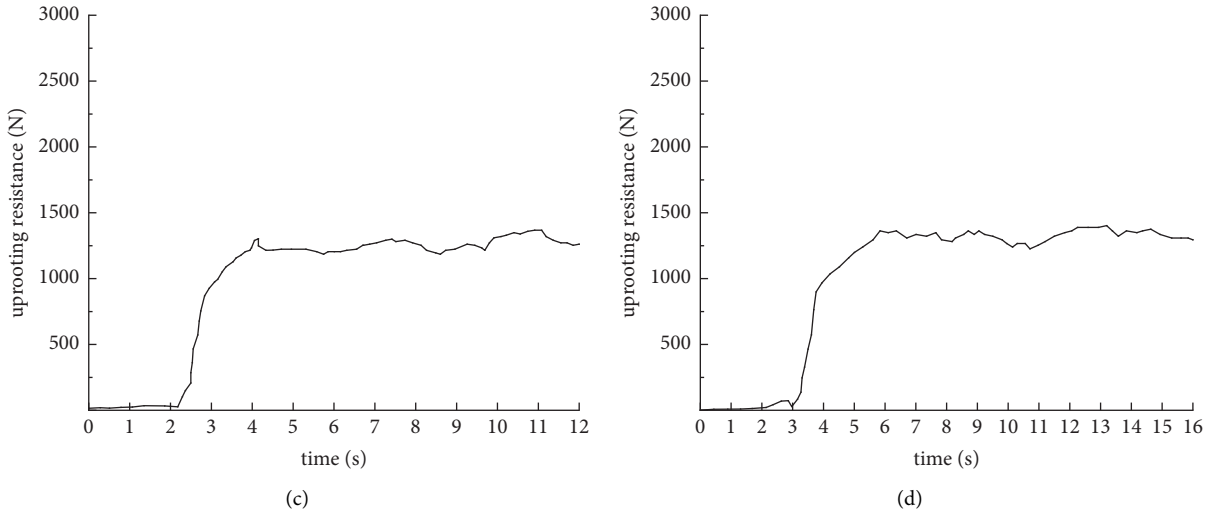

Figure 11: Sand matrix, double-layer stone test results. (a) Test 4-1. (b) Test 4-2. (c) Test 4-3. (d) Test 4-4.

Table 4: Tensile force representative value (N) of pull-out test.

Filler type	The thickness of the soil-rock mixture	1	2	3	4
Clay	Monolayer 10 cm	1950	1830	1650	1510
	Double-layer 20 cm	2720	1720	1800	1490
Sand	Monolayer 10 cm	1580	1450	1140	1300
	Double-layer 20 cm	1420	1340	1320	1390

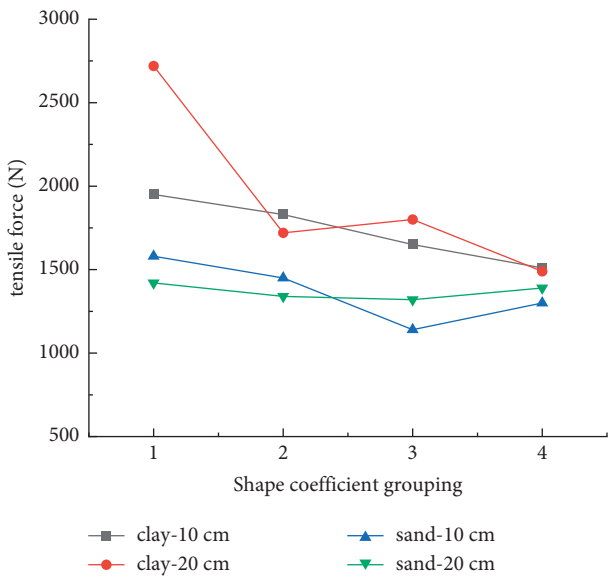

Figure 12: A representative value of tension in the pull-out test.

Table 5: Top plate inclination angle of pull test (°).

Filler type	The thickness of the soil-rock mixture	1	2	3	4
Clay	Monolayer 10 cm	8	8	6	6
	Double-layer 20 cm	12	11	11	6
Sand	Monolayer 10 cm	10	10	9	11
	Double-layer 20 cm	15	14	9	12

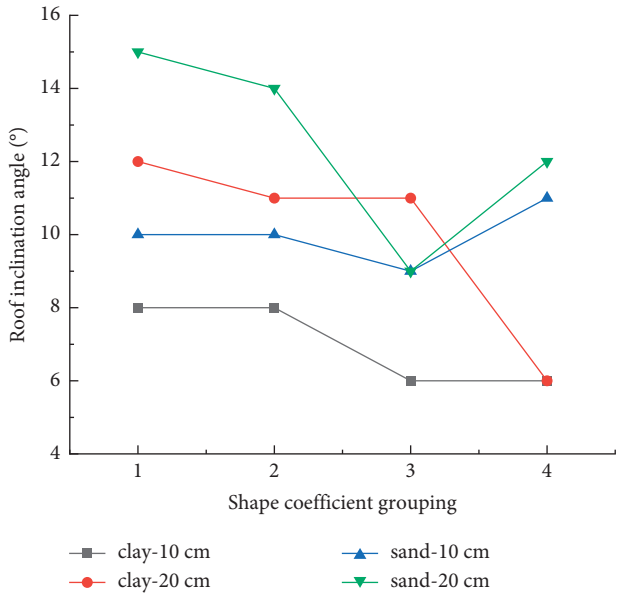

Figure 13: A representative value of tension in the pull-out test.

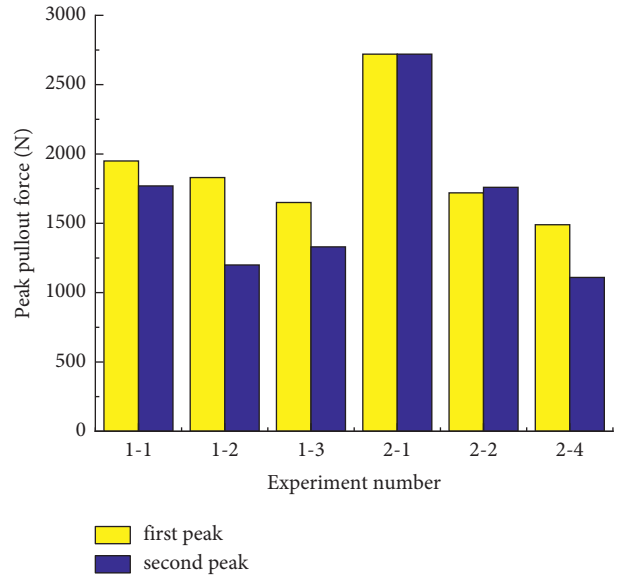

Figure 14: Comparison of peak values of clay matrix pull-out test.

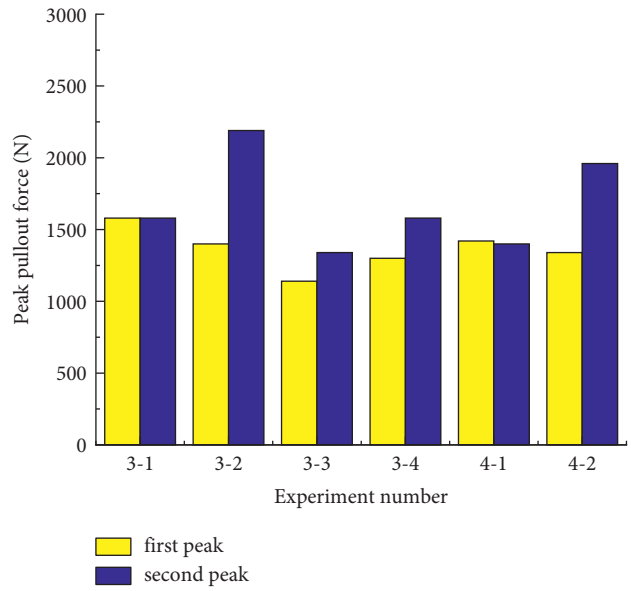

Figure 15: Comparison of peak values of sand matrix pull-out test.

single-layer soil-rock mixture is less than that of the double-layer soil-rock mixture.

During the 16 tests, the second peak appeared in 12 tests, and the time interval between the second peak and the first peak was about 5 seconds. From Figure 14, in the pull-out test with clay as the matrix, the second peak is lower than the first peak.

On the contrary, the second peak is higher than the first peak in the pull-out test with sand as a matrix (Figure 15).

This phenomenon is closely related to the end time of the test, and the second peak occurs earlier than the time when the electric push rod is off. Therefore, the appearance of the second peak is not caused by the change in the pull-out speed of the geogrid after the electric push rod stops working. There was no secondary peak in the clay and sand pull-out tests without stone, indicating that the secondary peak in the tensile curve was related to stone. Based on the above two points, it can be seen that the second peak appears as the geogrid pulls out, and the thickness of soil between the baffle in front of the model box and the soil-rock mixture decreases gradually. The geogrid carries the soil-rock mixture to impact the baffle in front of the model box and encounters resistance, which increases the drawing force of the geogrid. According to this conclusion, the second peak value will be a good indicator to describe the integrity of the geogrid and soil-rock mixture. Concerning the phenomenon that the first peak value of the drawing force is larger than the second peak value in the clay matrix, and the first peak value of the drawing force is smaller than the second peak value in the sand matrix, it can be concluded that the integrity of the soil-rock mixture with sand as the matrix is stronger than that of the soil-rock mixture with clay as the matrix.

5. Discussion

Based on the analysis of the above test results, the following conclusions can be drawn:

(i) with the increase of the shape factor of the rock material, the maximum pull-out resistance provided by the soil-rock mixture gradually decreases, during the test, the inclination angle of the top plate of the model box gradually decreased. The stone shape factor will affect the occlusion between the geogrid grid and the stone, with the increase of the shape factor of the stone, the probability of the stone and the geogrid occlusion decreases, and the quality of the occlusion deteriorates. It is worth noting that in tests 3-4 and 4-4, the representative values of the pull-out force are smaller than those of the sand-soil pull-out test as a reference. This shows that the stones in these tests not only did not provide resistance to the relative sliding between the geogrid

and the soil-rock mixture but also reduced the resistance of the geogrid to pull out.

(ii) The pull-out force of the double-layer soil-rock mixture is greater than that of the single-layer soil-rock mixture, and the soil-rock mixture with a thicker layer can provide greater pull-out resistance to the geogrid, the size of the pull-out resistance of the geogrid is not only related to the stones in direct contact with the geogrid, but also the stones at a distance of 5 cm from the surface of the geogrid can still have an indirect effect on the pull-out resistance of the geogrid, the stone shape factor affects the mechanical occlusion between the stones in the soil-rock mixture, and this indirect effect weakens with the increase of the stone shape factor.

(iii) The representative value of the pull-out force in the soil-rock mixture with clay as filler is greater than that in the soil-rock mixture with sand as a filler. The representative value of the drawing force in the soil-rock mixture with sand as the matrix is 6%–20% less than that of the soil-rock mixture with clay as the matrix.

(iv) With the increase of the shape factor, the inclination angle of the roof of the model box in the clay matrix decreases gradually, and in the sand matrix, the roof of the model box decreases first and then increases, and the inclination angle of the roof of the model box with clay as filling material is less than that of the sand as filling material. In the test, the inclination angle of the roof of the single-layer soil-rock mixture is less than that of the double-layer soil-rock mixture.

(v) 2/3 of the test pull-out force curves showed a second peak, in which, the pull-out test with clay as the matrix, the second peak is lower than the first peak, while in the sand-based pull-out test the results are opposite, the second peak is higher than the first peak. Concerning the phenomenon that the first peak value of the drawing force is larger than the second peak value in the clay matrix, and the first peak value of the drawing force is smaller than the second peak value in the sand matrix, it can be concluded that the integrity of the soil-rock mixture with sand as the matrix is stronger than that of the soil-rock mixture with clay as the matrix. According to this conclusion, the second peak value will be a good indicator to describe the integrity of the geogrid and soil-rock mixture.

(vi) Through 16 pull-out tests, the following expression is obtained as an empirical expression, the geogrid pull-out test was performed to predict the pull-out force:

$$F = (56.2m - 47.8n - 91.2mn + 44.8)(S - 4.77) + 1258.6. \quad (7)$$

Data Availability

All data that support the findings of this study are available from the corresponding author upon reasonable request.

Conflicts of Interest

The authors declare that they have no conflicts of interest to report regarding the present study.

Acknowledgments

This work was supported by Beijing Natural Science Foundation (8214060) and National Natural Science Foundation of China (42107164).

References

[1] E. Medley and R. E. Goodman, "Estimating the Block Volumetric Proportions of Melanges and Similar Block-In-Matrix Rocks (Bimrocks) [C]," *north american rock mechanics symposium*, pp. 851–858, 1994.

[2] Z. P. Yang, S. Q. Li, Y. W. Jiang, Y. X. Hu, and X. R. Liu, "Shear mechanical properties of the interphase between soil-rock mixtures and benched bedrock slope surfaces [J]," *International Journal of Geomechanics*, vol. 22, no. 5, 2022.

[3] K. Cui and J. Xiang, "Effect of coarse grain content on the dynamic shear modulus and damping ratio of mixed soil under seismic load in western sichuan [J]," *China Journal of Highway and Transport*, vol. 32, no. 12, p. 123, 2019.

[4] X. P. Ji, B. Han, J. M. Hu, S. W. Li, Y. Xiong, and E. Y. Sun, "Application of the discrete element method and CT scanning to investigate the compaction characteristics of the soil-rock mixture in the subgrade," *Road Materials and Pavement Design*, vol. 23, no. 2, pp. 397–413, 2022.

[5] X. Yan, W. Zhan, Z. Hu, Y. Q. Yu, and D. Q. Xiao, "Experimental study on the effect of compaction work and defect on the strength of soil-rock mixture subgrade," *Advances in Materials Science and Engineering*, vol. 2021, pp. 1–13, 2021.

[6] F. H. Zhang, Z. R. Liu, Y. Chen et al., "Numerical simulation of mutually embedded settlement in miscellaneous fill [J]," *Advances in Civil Engineering*, vol. 2020, no. 4, pp. 1–10, 2020.

[7] D. Pitilakis, A. Anastasiadis, A. Vratsikidis et al., "Large-scale field testing of geotechnical seismic isolation of structures using gravel-rubber mixtures," *Earthquake Engineering & Structural Dynamics*, vol. 50, no. 10, pp. 2712–2731, 2021.

[8] G. Q. Yang, H. B. Liu, Y. T. Zhou, and B. L. Xiong, "Post-construction performance of a two-tiered geogrid reinforced soil wall backfilled with soil-rock mixture," *Geotextiles and Geomembranes*, vol. 42, no. 2, pp. 91–97, 2014.

[9] Z. L. Zhang, W. J. Xu, W. Xia, and H. Y. Zhang, "Large-scale in-situ test for mechanical characterization of soil-rock mixture used in an embankment dam," *International Journal of Rock Mechanics and Mining Sciences*, vol. 86, pp. 317–322, 2016.

[10] J. G. Fan, D. Y. Wang, and D. Qian, "Soil-cement mixture properties and design considerations for reinforced excavation," *Journal of Rock Mechanics and Geotechnical Engineering*, vol. 10, no. 4, pp. 791–797, 2018.

[11] H. Sonmez, E. Tuncay, and C. Gokceoglu, "Models to predict the uniaxial compressive strength and the modulus of elasticity for Ankara Agglomerate," *International Journal of Rock Mechanics and Mining Sciences*, vol. 41, no. 5, pp. 717–729, 2004.

[12] H. Sonmez, C. Gokceoglu, E. W. Medley, E. Tuncay, and H. A. Nefeslioglu, "Estimating the Uniaxial Compressive Strength of a Volcanic bimrock [J]," *International Journal of Rock Mechanics and Mining Sciences*, vol. 43, no. 4, pp. 554–561, 2006.

[13] E. W. Medley, "The Engineering Characterization of Melanges and Similar Block-In- Matrix Rocks (Bimrocks) [M]," University of California, Berkeley, 1994.

[14] A. A. Kalender, H. Sonmez, E. Medley, C. C. Tunusluoglu, and K. Kasapoglu, "An approach to predicting the overall strengths of unwelded bimrocks and bimsoils," *Engineering Geology*, vol. 183, pp. 65–79, 2014.

[15] L. jin, Y. zeng, L. xia, and Y Yang, "Experimental and Numerical Investigation of Mechanical Behaviors of Cemented Soil–Rock Mixture [J]," *Geotechnical and Geological Engineering*, vol. 35, no. 1, 2017.

[16] Z. P. Zhang, Q. Sheng, X. D. Fu, Y. Q. Zhou, J. H. Huang, and Y. X. Du, "An approach to predicting the shear strength of soil-rock mixture based on rock block proportion," *Bulletin of Engineering Geology and the Environment*, vol. 79, no. 5, pp. 2423–2437, 2020.

[17] E. Teijón-López-Zuazo, A. Vega-Zamanillo, M. A. Calzada-Pérez, and L. Juli-Gándara, "Estimation of unconfined compressive strength of cement-stabilized jabre as material upgrade on highway construction," *Materiales de Construcción*, vol. 70, no. 338, p. 218, 2020.

[18] M. Sonmez, A. Ercanoglu, G. Kalender, and C. Dagdelenler, "Predicting Uniaxial Compressive Strength and Deformation Modulus of Volcanic Bimrock Considering Engineering dimension [J]," *International Journal of Rock Mechanics & Mining Sciences*, pp. 91–103, 2016.

[19] Z. Shu, B. Liu, N. Liang, L. Yue, and D. Wang, "Study on the fractal characteristics of earth-rock coarse grain based on digital image processing [J]," *Chinese Journal of Underground Space and Engineering*, vol. 8, no. 3, pp. 511–489, 2012.

[20] Y. Wang, X. Li, B. Zheng, S. D. Li, and Y. T. Duan, "A laboratory study of the effect of confining pressure on permeable property in soil-rock mixture," *Environmental Earth Sciences*, vol. 75, no. 4, p. 284, 2016.

[21] V. R. Mawby, "Porosity Influence on the Shear Strength of Granular Material–clay mixtures [J]," *Engineering Geology*, vol. 58, no. 2, pp. 125–136, 2000.

[22] X. Liu, T. U. Yiliang, L. Wang et al., "Fractal Characteristics of Shear Failure Surface and Mechanism of Strength Generation of Soil-Rock aggregate [J]," *Chinese Journal of Rock Mechanics and Engineering*, vol. 36, no. 9, pp. 2260–2274, 2017.

[23] X. D. Lei, Z. P. Yang, X. J. Zhang, Y. L. Tu, and Y. X. Hu, "Shear properties and rock block breakage characteristics of soil-rock mixtures [J]," *Yantu Lixue/Rock and Soil Mechanics*, vol. 39, no. 3, pp. 899–908, 2018.

[24] C. Shi, I. J. S. Ba, Y. U. Shi-Yan, and W. Wang, "Meso-structural Characteristic and Random Reconstruction of Soil-Rock Particles Based on Plural Fourier analysis [J]," *Rock and Soil Mechanics*, vol. 37, no. 10, pp. 2780–2786, 2016.

[25] C. Shi and J. L. Shen, "Comparative Analysis for 3D Shape Characterization Parameters of Rock and Soil particles [J]," *Journal of Shenyang University of Technology*, vol. 39, no. 4, pp. 469–474, 2017.

[26] Q. Zhang, X.-G. Wang, Y.-F. Zhao, L. P. Liu, and X.-C. Lin, "3D random reconstruction of meso-structure for soil-rock mixture and numerical simulation of its mechanical characteristics by particle flow code [J]," *Yantu Gongcheng Xuebao/Chinese Journal of Geotechnical Engineering*, vol. 41, no. 1, pp. 60–69, 2019.

[27] N. Coli, P. Berry, D. Boldini, and R. Bruno, "The contribution of geostatistics to the characterisation of some bimrock properties," *Engineering Geology*, vol. 137-138, pp. 53–63, 2012.

[28] S. Y. Wang, G. X. Chen, L. K. Zhang, and J. Yuan, "Triaxial discrete element simulation of soil–rock mixture with different rock particle shapes under rigid and flexible loading modes," *International Journal of Geomechanics*, vol. 21, no. 8, 2021.

[29] J. Gong, J. Liu, and L. Cui, "Shear behaviors of granular mixtures of gravel-shaped coarse and spherical fine particles investigated via discrete element method," *Powder Technology*, vol. 353, pp. 178–194, 2019.

[30] Y. S. Yao, J. Li, J. J. Ni, C. H. Liang, and A. S. Zhang, "Effects of gravel content and shape on shear behaviour of soil-rock mixture: experiment and DEM modelling [J]," *Computers and Geotechnics*, vol. 141, 2022.

[31] D. Minuto and L. Morandi, *Geotechnical characterization and slope stability of a relict landslide in bimsoils (blocks in matrix soils) in dowtown genoa, Italy[M]*, Vol. 2, Engineering Geology for Society and Territory, Italy, 2015.

[32] F. M. Ezzein and R. J. Bathurst, "A new approach to evaluate soil-geosynthetic interaction using a novel pullout test apparatus and transparent granular soil," *Geotextiles and Geomembranes*, vol. 42, no. 3, pp. 246–255, 2014.

[33] G. Cardile, D. Gioffrè, N. Moraci, and L. S. Calvarano, "Modelling interference between the geogrid bearing members under pullout loading conditions," *Geotextiles and Geomembranes*, vol. 45, no. 3, pp. 169–177, 2017.

[34] M. Ennio and M. Palmeira, "Soil–geosynthetic interaction: modelling and analysis - ScienceDirect [J]," *Geotextiles and Geomembranes*, vol. 27, no. 5, pp. 368–390, 2009.

[35] D. Derksen, Z. Ziegler, and F. Fuentes, "Geogrid-soil interaction: a new conceptual model and testing apparatus," *Geotextiles and Geomembranes*, vol. 49, no. 5, pp. 1393–1406, 2021.

[36] G. Altay, C. Kayadelen, T. Taşkıran, and Y. Z. Kaya, "A laboratory study on pull-out resistance of geogrid in clay soil," *Measurement*, vol. 139, pp. 301–307, 2019.

[37] M. Y. Fattah, M. A. Yousif, and A. Rasheed, *Production of Waste Rubber-Made Geogrid Reinforcement for Strengthening Weak Soils*, pp. 265–278, Singapore, 2021.

[38] J. Q. Wang, Y. F. Zhou, L. U. Meng-Liang, and L. I. Liang, "Pull-out Test and Analysis on Geogrid Mechanical characteristics [J]," *Journal of Guangxi University (Natural Science Edition)* vol. 41, no. 1, pp. 134–140, 2016.

[39] R. Chen, M. T. Luan, W. Zhao, X. Y. Xu, and D. X. Hao, "Research on pull-out test and frictional resistance characteristic of geogrids [J]," *Rock and Soil Mechanics*, vol. 30, no. 4, pp. 960–964, 2009.

[40] M. X. Zhang, H. Zhou, A. A. Javadi, and Z. W. Wang, "Experimental and theoretical investigation of strength of soil reinforced with multi-layer horizontal-vertical orthogonal elements," *Geotextiles and Geomembranes*, vol. 26, no. 1, pp. 1–13, 2008.

[41] K. Kayadelen, T. O Onal, and A. Altay, "Experimental study on pull-out response of geogrid embedded in sand," *Measurement*, vol. 117, pp. 390–396, 2018.

[42] B. J. Nareeman and M. Y. Fattah, "Effect of soil reinforcement on shear strength and settlement of cohesive-frictional soil [J]," *International Journal of Geomate Geotechnique Construction Materials & Environment*, vol. 3, pp. 308–313, 2012.

[43] S. Adis, M. Senad, and I. Tomislav, "Numerical investigations of interaction between geogrid/wire fabric reinforcement and cohesionless fill in pull-out test [J]," *Građevinar*, vol. 72, no. 03, pp. 237–252, 2020.

[44] K. Park, D. Kim, J. Park, and H. Na, "The determination of pullout parameters for sand with a geogrid," *Applied Sciences*, vol. 11, no. 1, p. 355, 2020.

[45] Mr Abdi, Ar Zandieh, H. Mirzaeifar, and M. A. Arjomand, "Influence of geogrid type and coarse grain size on pull out behaviour of clays reinforced with geogrids embedded in thin granular layers," *European Journal of Environmental and Civil Engineering*, vol. 25, no. 12, pp. 2161–2180, 2021.

[46] A. Emran, O. Maher, S. Abdallah et al., "Geogrid bridging over existing shallow flexible PVC buried pipe-Experimental study [J]," *Tunnelling and Underground Space Technology*, vol. 113, 2021.

[47] Ge Gao and M. Meguid, "Effect of particle shape on the response of geogrid-reinforced systems: insights from 3D discrete element analysis," *Geotextiles and Geomembranes*, vol. 46, no. 6, pp. 685–698, 2018.

[48] C. Cheng, M. Glenn, and R. Rui, "Discrete Element Modelling of Geogrids with Square and Triangular apertures [J]," *Geomechanics and Geoengineering*, vol. 16, no. 5, pp. 495–501, 2018.

[49] J. F. Chen, L. I. Hui-Li, J. X. Liu, and J. Zhou, "Mesoscopic Study of Interface Properties of Geogrid-Reinforced soil [J]," *Rock and Soil Mechanics*, vol. 32, no. S1, pp. 66-, 2011.

[50] M. Ghazavi and O. Bavandpouri, "Analytical solution for calculation of pull out force-deformation of geosynthetics reinforcing unsaturated soils," *Geotextiles and Geomembranes*, vol. 50, no. 2, pp. 357–369, 2022.